Journal of Electrochemical Science and Technology
Vol. 2, No. 2, 2011, 68-75
http://dx.doi.org/10.5229/JECST.2011.2.2.068

Review

Journal of Electrochemical Science and Technology

Blocking Layers Deposited on TCO Substrate and Their Effects on Photovoltaic Properties in Dye-Sensitized Solar Cells

Beomjin Yoo[a], Kyungkon Kim[a], Doh-Kwon Lee[a], Hong Gon Kim[a], BongSoo Kim[a], Nam-Gyu Park[b], and Min Jae Ko[a,†]

[a]*Solar Cell Research Center, Korea Institute of Science and Technology, Seoul, 136-791, Korea*
[b]*School of chemical Engineering, Sungkyunkwan University, Suwon 440-746, Korea*

ABSTRACT :

In this review, we have investigated the effect of TiO_2-based blocking layers (t-BLs), deposited on a transparent conductive oxide (TCO)-coated glass substrate, on the photovoltaic performance of dye-sensitized solar cells (DSSCs). The t-BL was deposited using spin-coating or sputtering technique, and its thicknesses were varied to study the influence of the thin TiO_2 layer in between transparent conducting glass and nanocrystalline TiO_2 (nc-TiO_2). The DSSC with the t-BL showed the improved adhesion and the suppressed charge recombination at a TCO glass substrate than those without the t-BL, which led to the higher conversion efficiency.

Keywords: Dye-sensitized solar cell, Blocking layers, Transparent conducting oxides, Charge recombination, Adhesion properties

Received May 27, 2011 : Accepted June 3, 2011

1. Introduction

Dye-sensitized solar cells have been extensively studied since their discovery in 1991 by Grätzel's research group[1] because they have been considered as a good alternative to conventional silicon photovoltaic cells due to their low production costs and colorful characteristics. As a consequence of this special attention, DSSCs with energy conversion efficiencies higher than 11% have been obtained using nc-TiO_2 films having a mesoporous structure in conjunction with a liquid electrolyte.[2-4]

A DSSC is commonly comprised of a dye-bonded nc-TiO_2 film on a transparent conducting oxide glass as the anode, a liquid electrolyte containing the I_3^-/I^- redox couple and a Pt counter electrode as the cathode. The working principle of the DSSC is based upon the following primary steps (Fig. 1): the Ru(II)-bipyridine dye anchored on the TiO_2 surface absorbs the incident light through

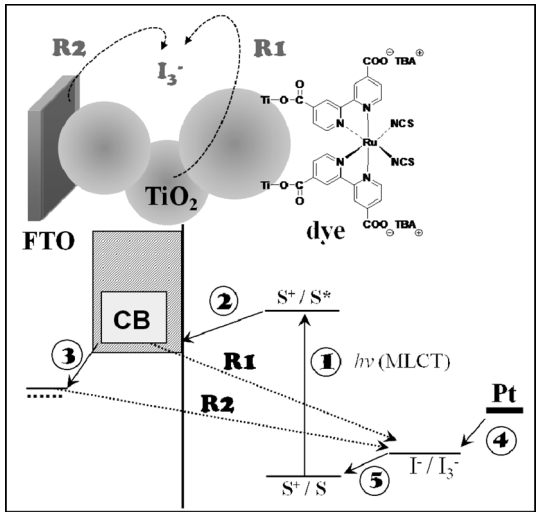

Fig. 1. Schematic diagram of electron transfer processes in a dye-sensitized solar cell: (1) photo-excitation of the Ru(II)-bipyridine dye; (2) injection of electrons; (3) diffusion and charge-collection of electrons; (4) reduction of the I_3^- ions; (5) regeneration of the oxidized dye (electron loss by recombination, R1 and R2).

†Corresponding author. Tel.: +82-2-958-5518
E-mail address: mjko@kist.re.kr

a glass substrate, the photoexcited dye injects the electrons to the TiO_2, and the photo-injected electrons in the conduction band of TiO_2 are transported through the interconnected nanoparticles of TiO_2 to the FTO as a charge collector. The transported electrons finally reach the Pt counter electrode through the external circuit, and the I_3^- ions in electrolyte are reduced by the oxidation of I^- ions. The regeneration of oxidized dye is caused by the oxidation of the I^- ions.

Since electron diffusion rate is as low as microsecond under the 1 sun illumination and TiO_2 particles are surrounded by electrolyte, photo-injected electrons may undergo recombination from the TiO_2 conduction band either to the electrolyte or to the oxidized dye. It was reported that electron loss by recombination can take place either at the nanocrystalline TiO_2/electrolyte interface in the bulk film (R1 of the Fig. 1) or at FTO substrate (R2 of the Fig. 1), where recombination has been believed to take place in general in the bulk film.[5-8] Afterward, it was argued that recombination occurs predominantly near the substrate instead of across the entire TiO_2 film from the intensity-modulated infrared transmittance measurements.[9] Recently, Cameron and Peter emphasized that charge recombination at FTO/electrolyte interface cannot be neglected.[10-12]

We have thus motivated to investigate the loss of photo-injected electrons at the TCO substrate/electrolyte interface in DSSC by means of blocking layers formed by spin-coating or sputtering technique.

In this study, we focused on the effect of introducing thin TiO_2 layer on TCO substrate as the blocking layer, and compared its performance with a cell without blocking layer in terms of the photovoltaic parameters and interfacial properties of the DSSCs.

2. Experimental

2.1. Conducting substrates fabrication

Chemically deposited t-BLs were prepared by spin-coating of the 1-butanol solution contained titanium(IV) bis(acetylacetonate) diisopropoxide ($Ti(acac)_2OiPr_2$ 75 wt.% in isopropanal) precursor on a FTO glass (Pilkington TEC8, ~8 Ω/ □ , 2.3 μm thick), followed by annealing at 500°C in air for 20 min. The concentration of the precursor solution was varied from 0.05 M to 0.2 M.

Transparent conducting substrates based on ITO/FTO/TiO_2 triple-layered structure were prepared on glass substrate by radio frequency (rf) magnetron sputtering method. An ITO layer with thickness of 150 nm was sputtered on a plain glass substrate (Quartz, JNC Ltd, NC-200) from ITO target (In_2O_3-SnO_2) which contained 10 wt.% SnO_2. Then, a FTO layer with thickness of 70 nm was deposited on the ITO layer by sputtering of SnO_2 target (99.99%) in gas mixtures of CF_4, O_2 and Ar. The substrate temperature was 300°C. Finally, the deposition process of sputtered-TiO_2 layer was carried out on the FTO-coated ITO layer by sputtering of TiO_2 target under O_2/Ar (3.5/96.5, v/v) flow ratio at a substrate temperature of 300°C.

2.2. DSSC fabrication

DSSCs were fabricated as follows: Transparent conducting substrates were pre-cleaned ultrasonically in ethanol. The nanocrystalline TiO_2 particles for the screen-printable paste were synthesized by hydrolyzing titanium tetraisopropoxide in the presence of acetic acid, followed by autoclaving at 230°C for 12 h.[13] The prepared nc-TiO_2 paste was deposited on the transparent conducting glasses, dried in air at ambient temperature for 5 min and sintered at 500°C for 30 min.

The thicknesses of resulting TiO_2 films were measured by an Alpha-step IQ surface profiler (KLA Tencor), and were determined to be about 10 μm and 5 μm for the FTO and ITO/FTO substrate, respectively.

For dye adsorption, the sintered nc-TiO_2 electrodes were immersed in absolute ethanol containing 0.5 mM of N-719 dye ($Ru[LL'(NCS)_2]$, where L = 2,2'-bypyridyl-4,4'-dicarboxylic acid, L' = 2,2'-bypyridyl-4,4'-ditetrabutylammonium carboxylate) for 5 hr at 40°C. A Pt counter electrode was prepared by thermal reduction of thin film formed from 7 mM of $H_2PtCl_6 \cdot 6H_2O$ in 2-propanol at 400°C for 20 min. The dye-adsorbed nc-TiO_2 electrode and Pt counter electrode were assembled using 60 μm-thick surlyn (Dupont 1702). An electrolyte solution was introduced through a drilled hole on the counter electrode, where the electrolyte solution was composed of 0.7 M 1-propyl-3-methyl imidazoliuim iodide (PMII), 0.03 M I_2, 0.05 M guanidinium thiocyanate (GuSCN) and 0.5 M 4-*tert*-butylpyridine in the mixture of acetonitrile and valeronitrile (v/v 85 : 15). The active areas of dye-coated TiO_2 films were measured by an image analysis program equipped with a digital microscope camera (Moticam 1000).

2.3. Measurements

Transmittance spectra for the transparent conducting glasses were recorded using a Perkin-Elmer Lambda

35 UV/Vis spectrometer. The cross section and surface morphologies of the transparent conducting substrates were measured by a field emission scanning electron microscope (NOVA-SEM). AFM images were recorded under room temperature conditions in a commercial AFM (Asylum Research MFP3D) in non-contact mode (AC mode) with 10 nm standard cantilevers (AC160TS, Olympus). The measurement of the atomic concentration depth profile was also carried out with an Auger electron spectroscopy (AES, Scanning Auger Nanoprobe PHI-700 & LC-TOFMS LECO). The depth profile of an ITO/FTO/TiO_2 conducting glass was obtained with ion beam sputtering when the etching rate was 15 nm/min (estimated with SiO_2). The electrochemical impedance spectra were measured with a potentiostat (Solartron 1287) equipped with a frequency response analyzer (Solartron 1260), with the frequency ranging from 10^{-2} to 10^6 Hz. The magnitude of the alternative signal was 10 mV. Impedance parameters were determined by fitting of impedance spectrum using Z-view software.

Photocurrent-voltage measurements were performed using a Keithly model 2400 source measure unit. A class-A solar simulator (Yamashita Denso, model YSS-200A) equipped with a 1600 W Xenon lamp was used as a light source, where light intensity was adjusted using a Fraunhofer ISE-calibrated mono Si solar cell with KG-3 filter for approximating AM 1.5 G one sun light intensity.

For the transient photocurrent and photovoltage studies, the cells were probed with a weak laser pulse at 532 nm superimposed on a relatively large and background (bias) illumination at 680 nm.[14,15] The bias light was illuminated by a 0.5 W diode laser (B&W TEK Inc., Model : BWF1-670-300E/55370). A 30 mW frequency-doubled Nd : YAG laser (Laser-Export Co. Ltd. Model : LCS-DTL-314QT) (λ = 532 nm, pulse duration 10 ns) was used as probe light. The light intensity of the probe light was adjusted so that the collected charge due to the transient photocurrent and photovoltage were less than 1% of the steady-state charge as estimated from the product of the steady-state short-circuit photocurrent/voltage, the time constant for electron collection (τ_C), and the time of electron life time (τ_R). Charge collection efficiency was estimated by the relation $\eta_{CC} = 1 - (\tau_C/\tau_R)$.[16]

3. Results and Discussion

3.1. FTO/t-BLs conducting substrates

Fig. 2 shows surface and cross-section SEM micrographs of bare FTO and blocking layer-deposited FTO glasses. From the surface SEM micrographs, the FTO surface structure becomes less clear as increasing the Ti precursor concentration, indicating that the increase in the precursor concentration leads to the increase in the TiO_2 blocking layer thickness. Based on this observation, it is thought that the compact blocking layer film could be obtained until the precursor solution concentration lower than 0.1 M, and the porous film structures were obtained on the compact thin layer above the precursor concentration of 0.1 M.

Fig. 2 also shows the dependency of short-circuit photocurrent density (J_{SC}), open-circuit voltage (V_{OC}), fill factor (*FF*) and efficiency (η) on the Ti precursor concentration. Photocurrent density increased with the precursor concentration, reached maximum at around 0.15 M. It decreased with increasing further Ti precursor concentration. The open-circuit voltages are also slightly improved by introduction of blocking layer. The V_{OC} of 0.788 V is enhanced to approximately 0.794 V after formation of blocking layers. Compared with the cell without blocking layer, fill factor is improved a bit after deposition of blocking layers. As a result, the overall conversion efficiency increases from 7.2% without blocking layer to 7.71% with 0.15 M-based blocking layer, corresponding to 7.1% increment. It was reported that the sputter-deposited blocking layers on FTO improved transmittance of visible light, which was responsible for the increased photocurrent.[17] Hence, optical effect may not be ruled out.

Fig. 3(a) compares the dark current characteristics of nanocrystalline TiO_2 electrodes with and without blocking layer. The onsets of the dark currents shift to higher forward bias voltage after formation of the blocking layers. There are two major contributions for dark current : one is contribution from the FTO/electrolyte interface and the other from the TiO_2/electrolyte one.[18,19] Since we used the same TiO_2 layer, there will be little change in the TiO_2/electrolyte interface in our experiment. Therefore, the interfaces between the exposed FTO and electrolyte are responsible for the dark current. The dark currents are decreased similarly after formation of blocking layers, which implies that the FTO surfaces exposed to electrolyte are well covered, regardless of the precursor concentration. The decreased dark current, irrespective of blocking layer thickness in this work, is consistent with the previous result,[17] where dark currents were reduced to same extent regardless of thickness of titania blocking layer formed by sputtering method. This indicates that blocking layer has unidirectional effect.

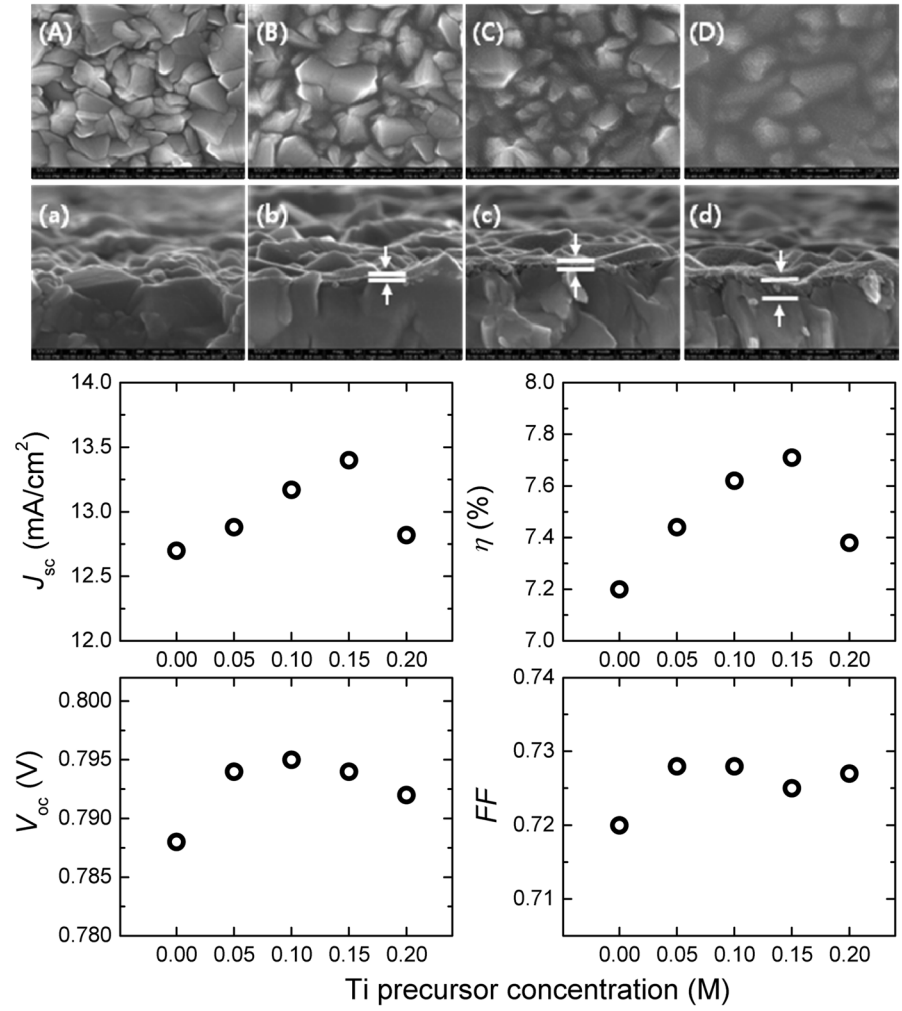

Fig. 2. Surface (A-D) and cross-section (a-d) SEM micrographs for the bare FTO, blocking layer-deposited FTO substrates from the Ti precursor solutions with various concentration. Effect of the Ti precursor concentration for the blocking layers on J_{SC}, V_{OC}, *FF* and η.

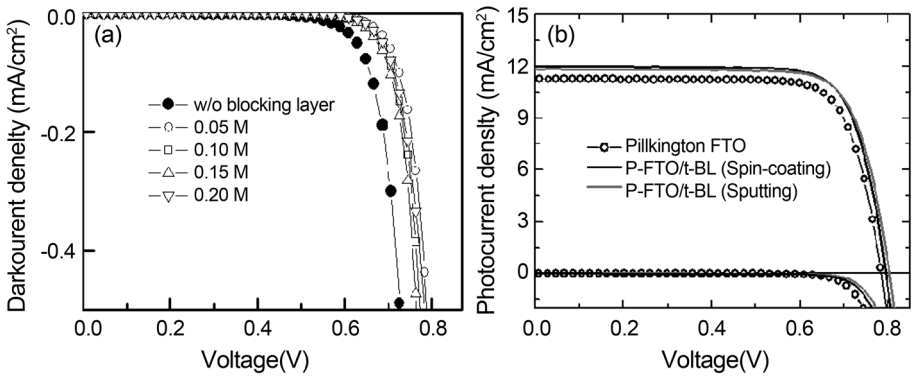

Fig. 3. (a) Dependence of dark current density on the Ti precursor concentration for the blocking layers. (b) Effect of the sputtered TiO_2 layer in FTO structure on (a) photocurrent and voltage and (b) dark current and voltage.

Fig. 3(b) compares the *J-V* curves of the three DSSCs fabricated with the FTO, FTO/t-BL (spin-coating method), FTO/t-BL (sputtering method) substrates, respectively. The photovoltaic parameters are summarized in Table 1. It is noted that the DSSCs with the FTO/t-BL substrates exhibited higher $V_{oc,}$ J_{sc}, and fill factors (FFs) than those with the FTO substrate. The onsets of the dark currents decreased similarly after formation of the t-BL, indicating that such a thin TiO_2 film protected back electron transfer.

3.2. ITO/FTO/TiO_2 conducting substrates

From the SEM micrograph in Fig. 4(a), ITO shows the thickness of about 150 nm with a large grain structure, while FTO exhibits a columnar structure and its thickness is about 70 nm. A clear distinction of the very thin TiO_2

Table 1. Photocurrent-Voltage characteristics of dye-sensitized solar cells[a] based on the FTO/t-BLs conducting glasses, along with the conventional FTO glass for comparison

Transparent conducting glasses	J_{SC} (mA/cm^2)	V_{OC} (V)	FF	η (%)	Area (cm^2)
Pilkington FTO	11.23	0.785	0.774	6.83	0.306
P-FTO/t-BL (Spin-coating)	11.83	0.803	0.772	7.33	0.317
P-FTO/t-BL (Sputtering)	12.00	0.795	0.771	7.35	0.298

[a]Photocurrent and voltage were measured with an aperture mask under AM 1.5 G one sun light intensity (100 mW/cm^2).

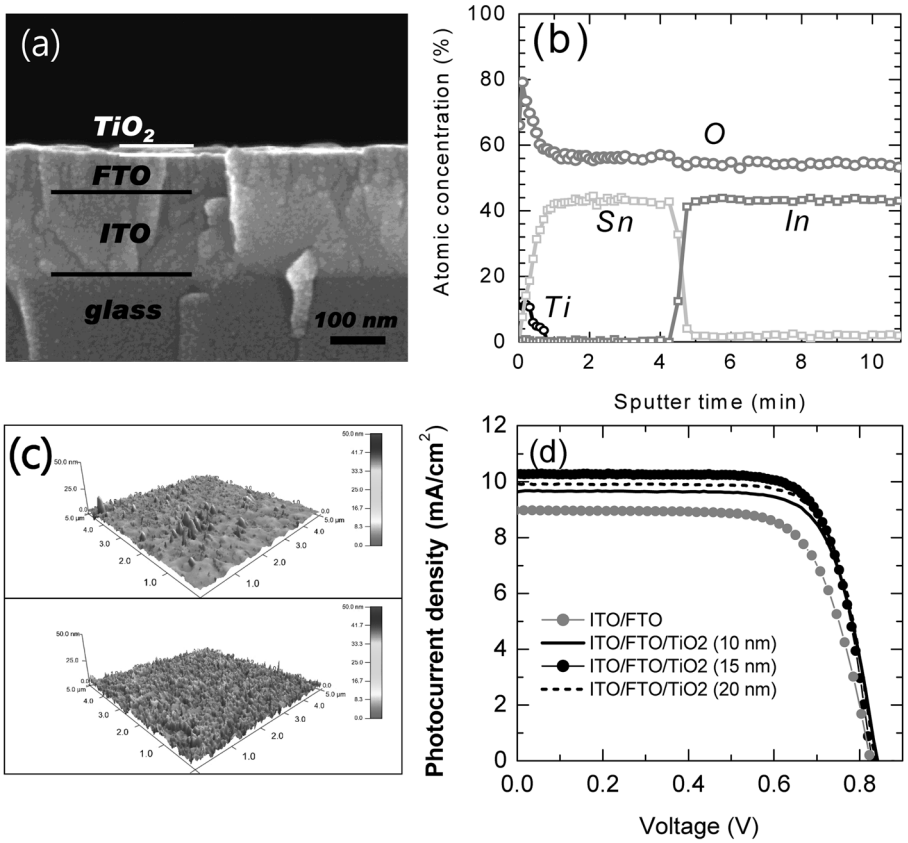

Fig. 4. (a) Cross-sectional view of SEM micrograph and (b) Auger electron spectroscopy (AES) depth profile of Ti, Sn, In and O atoms for the ITO/FTO/TiO_2 (15 nm) film. (c) Atomic force microscopy (AFM) images of FTO surface and 15 nm-thick-TiO_2-coated FTO surface in the ITO/FTO substrates. (d) Photocurrent-voltage curves of dye-sensitized solar cells based on the ITO/FTO/TiO_2 (*x* nm) conducting glasses.[20)]

layer is not easy from the SEM micrograph. However, we confirm the existence of TiO_2 layer and its thickness from the AES depth profile, as can be seen in Fig. 4(b). Considering the ion beam etching rate of about 20 nm/min, the TiO_2 layer is estimated to be about 16 nm. The FTO layer thickness is estimated to be about 74 nm from AES measurement, which is in good agreement with the SEM result. Fig. 4(c) shows the AFM images for the FTO surface in an ITO/FTO substrate and the 15 nm-thick TiO_2-coated FTO surface in an ITO/FTO/TiO_2 one. The root-mean-square roughness of the ITO/FTO sample and the ITO/FTO/TiO_2 one is about 1.41 nm and 1.82 nm, respectively, which indicates that the thin TiO_2 layer deposition does not significantly alter the roughness of FTO layer. Although there is little change in roughness, the surface with sparsely formed projections is changed to be densely formed ones by TiO_2 deposition.

Fig. 4(d) compares the photovoltaic performance of the ITO/FTO conducting glasses with and without the thin TiO_2 layer. Photocurrent density is substantially improved after deposition of thin TiO_2 layer on the top of FTO, while photovoltage remains almost unchanged. For the thin TiO_2 underlayer thickness, photocurrent density increases with increasing thickness, reached maximum at 15 nm and slightly decreases after further increase in thickness. Moreover, fill factor is improved after thin TiO_2 underlayer deposition, which is indicative of decrease in series resistance. As a consequence of the introduction of thin TiO_2 layer, overall conversion efficiency is improved from 5.28% to 6.37% upon 15 nm-thick TiO_2 deposition, corresponding to 20.6% increment.

Fig. 5(b) shows IPCE spectra before and after thin TiO_2 underlayer deposition. IPCE values are improved in the entire wavelength range. The increased IPCE may be due to an improved transmittance by insertion of thin TiO_2 underlayer. Fig. 5(a) shows UV-Vis spectra of the ITO/FTO/TiO_2 conducting glasses as a function of wavelength, along with the ITO/FTO one. Since the real system contains redox electrolyte, which is wet condition, we have compared the transmittance measured under the same wet condition. The samples for transmittance measurement were prepared as follows. The ITO/FTO and ITO/FTO/TiO_2 substrates were sealed with bare glasses using a 25 μm-thick surlyn and the same electrolyte used for dye-sensitized solar cell in this study was filled in between the TCO and the bare glass. The ITO/FTO conducting layers coated with thin TiO_2 layers with thickness ranging from 10-20 nm show higher transmittance at 300-600 nm range, whereas almost no difference was observed at 600-800 nm. Therefore, it cannot be ruled out that the increased photocurrent density is partly due to the increased transmittance. However, when comparing the optical transmittance with IPCE in Fig. 5(b), the increased IPCE at 600-800 nm cannot be explained by only transmittance change because there is no gain of optical transmittance at this wavelength range.

In Fig. 5(c) and (d), we plot transmittance and IPCE at 520 nm and at 650 nm. The increase in IPCE at 520 nm is closely related to the increased transmittance, while the change in IPCE at 650 nm is hardly related to the transmittance change. It can be said that the increased IPCE, associated with photocurrent density, is due to the increased transmittance at short wavelength range between 300-600 nm. However, at wavelength ranging

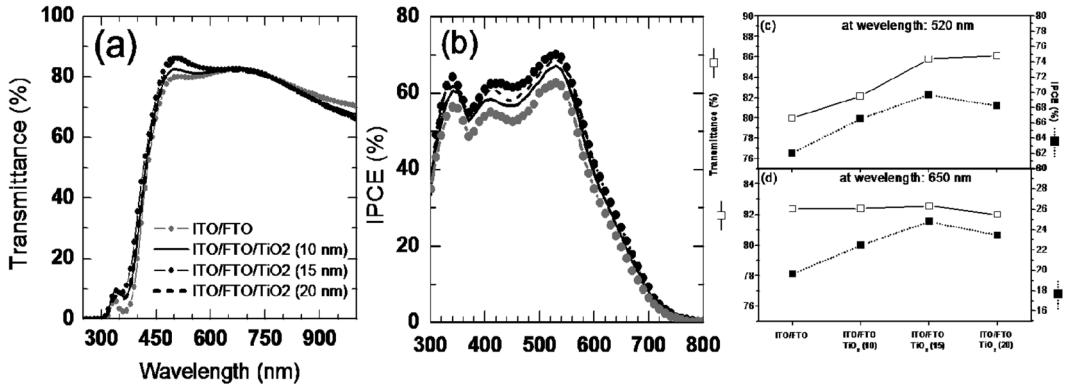

Fig. 5. (a) Optical transmittance and (b) IPCE spectra as a function of wavelength for the dye-sensitized solar cells based on the ITO/ATO/TiO_2 and the FTO substrates. Plot of transmittance (open circle) and IPCE (filled circle) at (c) 520 nm and (d) 650 nm.[20]

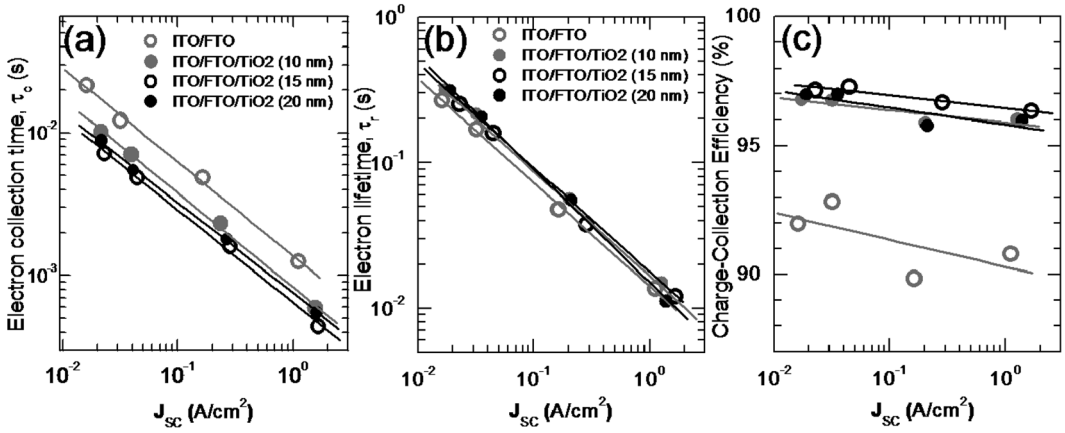

Fig. 6. Effect of the thin TiO_2 layers in the conductive ITO/FTO/TiO_2 structure on (a) the time constant for electron transport (τ_C) at short circuit condition, (b) the time constant for recombination (τ_R) at open circuit condition, and (c) charge collection efficiency (η_{CC}) as a function of light intensity, represented by the photocurrent density.[20]

from 600-800 nm, the increased IPCE is not related to the transmittance change, which implies that except for the optical gain other reason is involved for the increased photocurrent upon thin TiO_2 underlayer deposition.

Fig. 6 shows time constant for electron transport (τ_C), time constant for charge recombination (τ_R) and charge collection efficiency (η_{CC}) as a function of light intensity, represented by photocurrent density for the ITO/FTO and the ITO/FTO/TiO_2 substrate-based DSSCs. Charge collection efficiency is estimated using the relation of $\eta_{CC} = 1 - (\tau_C/\tau_R)$. Thin TiO_2 deposition on FTO improves electron transport rate, while it does not affect significantly charge recombination rate. As a result, charge collection efficiency is improved from ~90% to ~97% after formation of thin 15 nm-thick TiO_2 layer. Considering that the major alteration is observed from τ_C rather than τ_R by thin TiO_2 deposition, the improved charge collection efficiency is mainly due to the improved electron transport. Based on the observations from optical and transient photocurrent measurements, the thin insulating layer on the ITO/FTO conductive substrate is found to improve transmittance of the substrate, electrical contact at FTO and electron transport in TiO_2 film, leading to increase in photocurrent density.

4. Conclusions

We have studied the influence of the thin TiO_2 layer, deposited on a TCO conductive substrate, on photovoltaic property of dye-sensitized solar cell (DSSC) and prepared novel conducting substrates based on ITO/FTO for high efficiency dye-sensitized solar cell.

The DSSC with the TiO_2-based blocking layer prepared by sputtering or spin-coating deposition exhibited an enhanced photovoltaic parameters compared to the DSSC without the blocking layer on TCO glass substrate. Among these enhancements, photocurrent and fill factor were significantly influenced, whereas photovoltage was increased slightly after formation of blocking layer. The improved photocurrent partly came from the increased transmittance. Besides, from the transient photocurrent and photovoltage study, we found that electron transport rate was accelerated and thereby charge collection efficiency was substantially improved by the thin layer formed on TCO substrate.

The FF and V_{OC} enhancements were attributed to the improved adhesion between TCO/TiO_2 film and the suppression of charge recombination at the TCO/electrolyte interface, respectively.

Acknowledgment

This work was supported by the New & Renewable Energy of the Korea Institute of Energy Technology Evaluation and Planning (KETEP) grant (Grant No. 2009301001002E and 2010T100100654) funded by the Korea government Ministry of Knowledge Economy.

References

1. B. O. Regan and M. Grätzel, *Nature*, **353,** 737 (1991).
2. Y. Chiba, A. Islam, Y. Watanabe, R. Komiya, N. Koide and L. Han, *Jpn. J. Appl. Phys. Part 2.*, **45**, L638 (2006).

3. F. Gao, Y. Wang, D. Shi, J. Zhang, M. Wang, X. Jing, R. Humphry-Baker, P. Wang, S. M. Zakeeruddin and M. Grätzel, *J. Am. Chem. Soc.*, **130**, 10720 (2008).
4. N.-G. Park and K. Kim, *Phys. Stat. Sol. (a)*, **205**, 1895 (2008).
5. N. Kopidakis, J. van de Lagemaat and A. J. Frank, *Coord. Chem. Rev.*, **248**, 1165 (2004).
6. J. van de Lagemaat, N.-G. Park and A. J. Frank, *J. Phys. Chem. B*, **104**, 2044 (2000).
7. J. Bisquert, G. Garcia-Belmonte, F. Fabregat-Santiago, N. S. Ferriols, P. Bogdanoff and E. C. Pereira, *J. Phys. Chem. B*, **104**, 2287 (2000).
8. F. Pichot, S. Ferrere, C. L. Fields and B. A. Gregg, *J. Phys. Chem. B,* **105**, 1422 (2001).
9. K. Zhu, E. A. Schiff, N.-G. Park, J. van de Lagemaat and A. J. Frank, *Appl. Phys. Lett*., **80**, 685 (2002).
10. P. J. Cameron and L. M. Peter, *J. Phys. Chem. B*, **107**, 14394 (2003).
11. P. J. Cameron and L. M. Peter, *J. Phys. Chem. B*, **109**, 930 (2005).
12. P. J. Cameron and L. M. Peter, *J. Phys. Chem. B*, **109**, 7392 (2005).
13. H.-J. Koo, J. Park, B. Yoo, K. Yoo, K. Kim and N.-G. Park, *Inorg. Chim. Acta,* **361**, 677 (2008).
14. N. Kopidakis, K. D. Benkstein, J. van de Lagemaat and A. J. Frank, *J. Phys. Chem. B,* **107**, 11307 (2003).
15. K. D. Benkstein, N. Kopidakis, J. van de Lagemaat and A. J. Frank, *J. Phys. Chem. B,* **107**, 7759 (2003).
16. A. J. Frank, N. Kopidakis and J. van de Lagemaat, *Coord, Chem. Rev.,* **248**, 1165 (2004).
17. J. Xia, N. Masaki, K. Jiang and S. Yanagida, *J. Phys. Chem. B,* **110**, 25222 (2006) .
18. M. K. Nazeeruddin, A. Kay, I. Rodicio, R. Humphry-Baker, E. Mueller, P. Liska, N. Vlachopoulos and M. Grätzel, *J. Am. Chem. Soc*., **115**, 6382 (1993).
19. M. Dürr, A. Yasuda and G. Nelles, *Appl. Phys. Lett*., **89** 061110-1 (2006).
20. B. Yoo, K. Kim, D.-K. Lee, M. J. Ko, H. Lee, Y. H. Kim, W. M. Kim and N.-G. Park, *J. Mater. chem.*, **20**, 4392 (2010).